A model for meteoritic and lunar ^{40}Ar/^{39}Ar age spectra: Addressing the conundrum of multi-activation energies

P. Boehnke [a,*], T. Mark Harrison [a], M.T. Heizler [b], P.H. Warren [a]

[a] *Department of Earth, Planetary and Space Sciences, University of California, Los Angeles, CA 90095, United States*
[b] *New Mexico Bureau of Geology and Mineral Resources, Socorro, NM 87801, United States*

A B S T R A C T

Results of whole-rock ^{40}Ar/^{39}Ar step-heating analyses of extra-terrestrial materials have been used to constrain the timing of impacts in the inner solar system, solidification of the lunar magma ocean, and development of planetary magnetic fields. Despite the importance of understanding these events, the samples we have in hand are non-ideal due to mixed provenance, isotopic disturbances from potentially multiple heating episodes, and laboratory artifacts such as nuclear recoil. Although models to quantitatively assess multi-domain, diffusive ^{40}Ar* loss have long been applied to terrestrial samples, their use on extra-terrestrial materials has been limited. Here we introduce a multi-activation energy, multi-diffusion domain model and apply it to ^{40}Ar/^{39}Ar temperature-cycling, step-heating data for meteoritic and lunar samples. We show that age spectra of extra-terrestrial materials, the Jilin chondrite (K-4) and Apollo 16 lunar breccia (67514, 43), yielding seemingly non-ideal behavior commonly interpreted as either laboratory artifacts or localized shock heating of pyroxene, are meaningful and can be understood in context of the presence of multi-diffusion domains containing multiple activation energies. Internally consistent results from both the meteoritic and lunar samples reveal high-temperature/short duration thermal episodes we interpret as due to moderate shock heating.

© 2016 Elsevier B.V. All rights reserved.

1. Introduction

The use of extraterrestrial materials in the pioneering development of the ^{40}Ar/^{39}Ar age spectrum method (Merrihue, 1965; Merrihue and Turner, 1966) naturally followed from both the cosmochemical community's awareness of the benefits of coupling neutron irradiation with incremental laboratory degassing (Jeffery and Reynolds, 1961) and the mineralogic stability of extraterrestrial samples during vacuum heating. Indeed, application of early interpretative models for ^{40}Ar/^{39}Ar step-heating results (Turner et al., 1966) were confined to the extraterrestrial domain as the preferred minerals for use in terrestrial K–Ar dating were dominantly hydrous (biotite, muscovite, hornblende) which tended to yield complex age spectra during their breakdown in vacuo (e.g., Dalrymple and Lanphere, 1971; Lanphere and Dalrymple, 1971). Through the 1970s, geochronologists tended to prefer rule-based age spectrum interpretations (e.g., Dalrymple and Lanphere, 1974; Fitch et al., 1976) over the diffusion models favored by their extraterrestrial counterparts (e.g., Huneke, 1976; Wang et al., 1980).

This began to reverse through the 1980s as analytical methods and laboratory heating apparatus improved sufficiently to permit routine recovery of both age and kinetic information from anhydrous terrestrial phases (e.g., Lovera et al., 1989). In time, quantitative models of Ar isotope behavior in silicates became essentially the exclusive domain of geochronologists (e.g., Lee, 1995; Lovera et al., 1991, 2002).

An important interpretive advance in interrogating ^{40}Ar/^{39}Ar step-heating data over the past 30 years was the advent of the multi-diffusion domain (MDD) model (Lovera et al., 1989, 1991). This approach permits quantitative reconstruction of the thermal history experienced by a sample with a single site for parent potassium within a distribution of domain sizes – a likely property of most silicates (see McDougall and Harrison, 1999). There are two distinct sources of information available from an ^{40}Ar/^{39}Ar step-heating experiment; the age spectrum and associated Arrhenius plot. The age spectrum is calculated from the flux of radiogenic Ar (^{40}Ar*) relative to reactor produced Ar (^{39}Ar) that is released during discrete laboratory heating steps. The Arrhenius plot is derived by plotting diffusion coefficients (calculated from inversion of the ^{39}Ar release function assuming a single diffusion length scale) against the inverse absolute temperature of laboratory heating yielding estimates of the activation energy (E) and

frequency factor (D_o/r^2), and the size (ρ) and volume fraction (ϕ) of diffusion domains present. Sensible correlations between age and Arrhenius spectra show that Ar diffusion can occur by the same mechanisms in nature as in the laboratory (Lovera et al., 2002; Harrison and Lovera, 2014). The MDD model is broadly applicable to those phases that experienced diffusive loss of ^{40}Ar in nature, but remain stable during laboratory vacuum heating (e.g., feldspars and pyroxenes).

Despite the wide range of grain size expected in lunar and meteoritic samples, MDD theory was not utilized in a cosmochemical context until recently (Shuster et al., 2010; Shuster and Cassata, 2015). With rare exception (e.g., Albarède, 1978), extraterrestrial materials are complex multi-mineralic aggregates and thus require consideration of simultaneous degassing of Ar isotopes originating from multiple potassium sites with differing activation energies. These potential complications are particularly salient given that whole-rock ^{40}Ar/^{39}Ar step-heating analyses of these materials have been widely used to constrain the impact history of the inner solar system (Norman et al., 2006), when the lunar magma ocean crystallized (Dominik and Jessberger, 1978), and the timing of planetary magnetic fields (e.g., Shea et al., 2012).

Historically, explanations for the non-ideal age spectra of extraterrestrial materials either invoke recoil redistribution and/or loss (e.g., Turner and Cadogan, 1974) or mixing of different age clasts (Dominik and Jessberger, 1978). Unfortunately, neither hypothesis has any falsifiability and therefore have not been rigorously tested. More recently, Cassata et al. (2010) performed MDD modeling on ALH84001, a Martian meteorite, and explored the existence of a "kinetic crossover" between Ar diffusion in plagioclase and pyroxene to explain aspects of the age spectrum (apparently unaware that a model for ^{40}Ar diffusion in samples containing multiple activation energies had previously been proposed by Harrison and McDougall, 1981 and generalized by Harrison et al., 1991) but dismissed the effect due to both the poor fit of their solution and the extreme temperatures required. Instead, they advocated for enhanced pyroxene degassing due to localized heating to explain their data. Based on a detailed investigation of ^{40}Ar diffusion in pyroxene, which revealed possible "bursting" during partial melting, Cassata et al. (2011) proposed shock induced localized heating of pyroxene to explain a class of meteorite ^{40}Ar/^{39}Ar age spectra, including results for the Jilin chondrite. As they did not attempt to obtain a quantitative fit to the age spectra, it remained unclear whether this mechanism is feasible and falsifiable.

In this paper, we seek to address these issues by providing the first MDD modeling approach for multi-phase samples with differing activation energies that returns viable solutions in terms of model misfit and physical conditions. We apply this model to ^{40}Ar/^{39}Ar step-heating results for two extraterrestrial samples – the Jilin chondrite (K-4) and Apollo 16 lunar breccia 67514,43. Using an optimization algorithm that calculates the best fits to both the Arrhenius plot and age spectrum, we show that simultaneous solutions for the temperature–time history of thermal episodes experienced by these chondrite and lunar samples can be achieved and potentially provide unique insights into shock histories.

2. Samples

2.1. Jilin chondrite K-4

The arrival of the Jilin chondrite in northwestern China in 1976 remains the largest meteorite fall ever recorded, with over two metric tonnes recovered. The Jilin petrography has been extensively discussed (e.g., JIGKMS, 1977); in brief, this ordinary chondrite is comprised of olivine, orthopyroxene and troilite, with lesser amounts of other sulphide minerals, clinopyroxene, oligoclase, and orthoclase. Chondrules up to 2 mm in diameter com-

prise about 15% (by volume) of the meteorite and are supported in a finer grained matrix (Wang et al., 1980). Textures indicate that this H5 meteorite experienced early thermal metamorphism (approximately 700–800 °C; Dodd, 1981) followed by moderate shock metamorphism (>950 °C, Dodd, 1981; 12–27 GPa, Xie et al., 2001), as evidenced by glassy veins, microcrystalline regions (JIGKMS, 1977), and moderate development of planar fractures (Xie et al., 2001).

Prior work showed that the Kirin chondrite experienced multiple thermal events that caused extensive diffusive loss of both ^{4}He and ^{40}Ar between ∼2.6 to ∼0.4 Ga (Wang et al., 1980; Harrison and Wang, 1981; Begemann et al., 1985; cf. Müller and Jessberger, 1985). ^{40}Ar/^{39}Ar step-heating results for a number of Jilin fragments were interpreted to reflect Ar degassing from both feldspars and clinopyroxene (Wang et al., 1980; Harrison and Wang, 1981; Müller and Jessberger, 1985).

2.2. Apollo 16 lunar breccia 67514,43

Sample 67514,43 was acquired from the vicinity of North Ray Crater in the lunar highlands by the Apollo 16 mission. We studied a thin section (67514,49) from its parent sample which shows a heavily brecciated but monomict, geochemically ferroan (Dowty et al., 1974) anorthosite. The dominant mineral, 88%, is plagioclase, accompanied by 10% pyroxene, 2% olivine, and <1% opaque oxides. EPMA analyses show the plagioclase is highly anorthitic (An$_{96-99}$). The pyroxene, as modified by subsolidus exsolution, consists dominantly of roughly 10-μm wide lamellae, with the low-Ca lamellae clustering near En$_{50}$Wo$_3$ and the high-Ca lamellae near En$_{36}$Wo$_{41}$. Olivine is uniformly Fo$_{39-41}$. Although a few mineral and lithic fragments remain essentially unbrecciated up to 0.5 mm across, most of the rock's volume has been comminuted into a highly porous groundmass of fragments less than 0.1 mm across (See Online Supplement). In places, elongate clumps of high mafic-silicate abundance appear to represent sheared and broken derivatives of individual roughly 0.1 mm^2 mafic silicate grains, suggesting that even in the comminuted groundmass the scale of mixing during brecciation was generally only at a scale of order 1 mm. This texture as well as the uniformly "ferroan" mineral compositions together imply that 67514,49 is a monomict breccia. As a ferroan anorthosite from Apollo 16, 67514,49 is indirectly linked to some of the most ancient Sm–Nd isochron ages obtained from the Moon (∼4.3 Ga; Borg et al., 2014). We are aware of no previous ^{40}Ar/^{39}Ar results for this sample.

3. Methods

We utilized a conventional double vacuum furnace attached to a MAP-215-50 rare gas mass spectrometer at the New Mexico Geochronology Research Laboratory. Blanks were determined by analyzing the same heating schedule without a sample in the furnace. We used an (^{40}Ar/^{36}Ar)$_0$ = 1 to correct for primordial Ar which generally had a <1% effect on age. Any inaccuracies in this correction are negligible given the scale of the disturbances we investigate. The sample was irradiated in the TRIGA reactor at the USGS Denver (DeBey et al., 2012) to a J factor of 0.014773(4). Correction factors for interfering nuclear reactions are: (^{39}Ar/^{37}Ar)$_{Ca}$ = 0.000690(2), (^{36}Ar/^{37}Ar)$_{Ca}$ = 0.0002724(1), (^{38}Ar/^{39}Ar)$_K$ = 0.01077(1), and (^{40}Ar/^{39}Ar)$_K$ = 0.00720(2). Neutron fluence was monitored with co-irradiated hornblende Hb3gr assuming an age of 1072 Ma (Jourdan et al., 2006). A full description of the methods can be found in Heizler et al. (1999).

3.1. Heating schedule

Since virtually every previous ^{40}Ar/^{39}Ar analysis of extraterrestrial samples has used a monotonic laboratory heating sched-

ule, some commentary regarding that used here is needed. In this study, we incorporated three cycled temperature routines into the heating schedule to gain maximum leverage in evaluating the presence of multiple activation energies while not unnecessarily lengthening analysis time. The three cycles begin at 600, 800 and, 1100 °C when two 50 °C step-downs occur in sequence (e.g., 600 to 550 and then 500 °C). Further, we utilized isothermal duplicates at high temperatures to ensure complete degassing. As we will demonstrate, the use of this approach is essential to extracting meaningful thermal histories from samples containing multiple activation energies (see Harrison et al., 1991). The full heating schedules are given in the supplementary materials.

3.2. Diffusion modeling

Fitting a domain size distribution with multiple activation energies is a complex optimization problem as more than 20 variables require adjustment (i.e., E, D_o/r^2, ρ, ϕ for typically six to twenty domain sizes). Although an automated approach has been shown to reliably retrieve values of E and D_o/r^2 for single-E samples via linear regression of the early heating steps of an Arrhenius plot (Lovera, 1992), this approach is not feasible when two or more activation energies are present. Other workers have sought to hand fit such data through trial and error (e.g., Cassata et al., 2010) and while illustrative examples of fits are possible, the complexity of the problem precludes finding an optimal solution. We chose to use a global optimization algorithm to simultaneously invert both age and Arrhenius spectra. The Adaptive Particle Swarm (Zhan et al., 2009) utilizes a flock of particles to explore parameter space. A particle is an object that moves through the parameter space and remembers its own best solution, as well as knowing the best solution any particle has found so far. The velocity of any one particle is calculated from the sum of the distances between the best solution for that particle and the overall best solution. This characteristic allows each particle to be influenced by its immediate and global environments. For a more in depth explanation we refer the reader to Kennedy and Eberhart (1995). Specifically, we utilize twenty particles initially randomly dispersed over a plausible parameter space with two thousand iterations of the algorithm.

In order to evaluate the fit of each candidate solution, we need a function to calculate the difference between the model fit and the laboratory data. We use a standard sum of squares measure (e.g., Gallagher, 2012) for both datasets. However this is complicated, as we have to fit both the age spectrum and Arrhenius plot. That is, the problem is one of multi-objective optimization (Deb, 2014). In theory, if the MDD model perfectly describes Ar diffusion in our sample, the best fit to the Arrhenius plot would be the best fit to the age spectrum. However in practice there is a continuous grain and sub-grain size distribution, while we can only model a discrete distribution due to computational limitations. Therefore, it is likely that our simplified model does not capture all of the detailed features in Ar release patterns from natural materials.

Given that we are optimizing two objective functions (i.e., the age and Arrhenius spectra), there is a continuum of best fit solutions to the joint objective function as improvements in one dimension lead to a worse result in the other. That is to say there exists a Pareto frontier (Deb, 2014) where a solution that better fits the Arrhenius plot will give a worse fit to the age spectrum and vice versa. This behavior arises because the objective function is a sum of two different fits to the dataset, therefore it is possible to have the same overall goodness of fit but optimize one fit (e.g., age fit) at the expense of the other (i.e., the Arrhenius fit). This tradeoff introduces additional uncertainty in the parameters of interest (e.g., heating temperature). While a full calculation of the uncertainties in our solution is not feasible at present due to
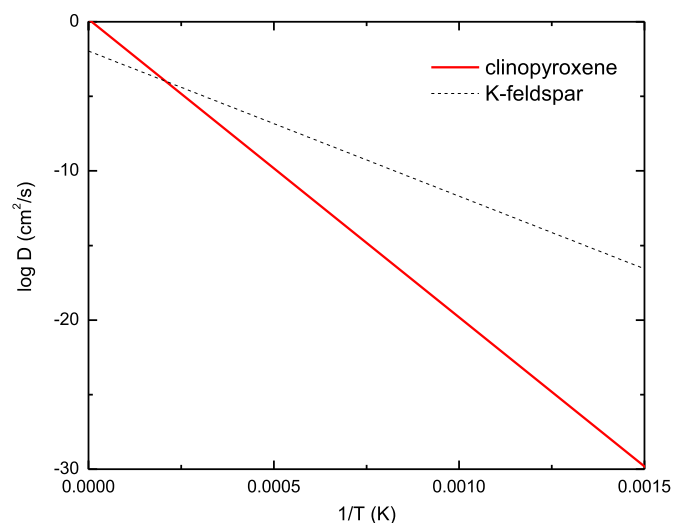

Fig. 1. This figure shows an example Arrhenius relation for both feldspar (Foland, 1974) and clinopyroxene (Cassata et al., 2011). The reversal in relative diffusivity occurring at high temperatures is referred to as a kinetic crossover.

the computational complexity, we instead present both the top 10 and 200 solutions to examine the range of viable solutions.

Our diffusion model uses the standard equations describing diffusive loss in a spherical geometry due to a re-heating event (Turner, 1968). The only modification to these equations is that we consider a summed release over multiple discrete domain sizes with differing activation energies. Our modeling is performed assuming $n = 20$ domain sizes for each E (and two activation energies in total) but virtually no change to the overall results occurs with more or less domain sizes down to $n = 4$. We did not model any data acquired at or above the temperature at which significant melting would occur (i.e., >1100 °C).

Given the vast dimension of parameter space, we used as much prior information as possible to limit the numerical range of the parameters. Activation energies for the low E phase were restricted between 20 and 60 kcal/mol, which encompasses the range of that determined for feldspars (e.g., Lovera et al., 1993; Cassata and Renne, 2013). For the high E phase, the range was constrained between 80 and 120 kcal/mol, again corresponding to that found for clinopyroxene (Cassata et al., 2011). The timing of both the reheating event and original formation are left as free parameters for the model but restricted to between present day and the 4.52 Ga gas retention age of the oldest known of H5 chondrites (Forest Vale; Turner et al., 1978).

4. Results

4.1. Analytical results

Our analysis of Jilin sample K-4 revealed, as before, a disturbed $^{40}Ar/^{39}Ar$ age spectrum (Fig. 2A) containing two distinct components; a high K/Ca and a low K/Ca phase. Following Wang et al. (1980), we interpret the high K/Ca phase as plagioclase and the low K/Ca phase as pyroxene. This interpretation is supported by our EPMA analyses of Jilin K-4, which yield an atomic K/Ca of 0.4 ± 0.1 for plagioclase (Supplement Table 1) which is consistent with the K/Ca determined from the Ar isotope measurements (Supplement Table 2; Fig. 2A).

We identify the portion of the age spectrum in which K/Ca drops from ∼0.2 to ∼0.001 as the transition to degassing dominated by clinopyroxene (∼72 to 100% ^{39}Ar released). This finding is supported by the Arrhenius plot (Fig. 3A) which shows that the low K/Ca phase is marked by a higher activation energy. The fact
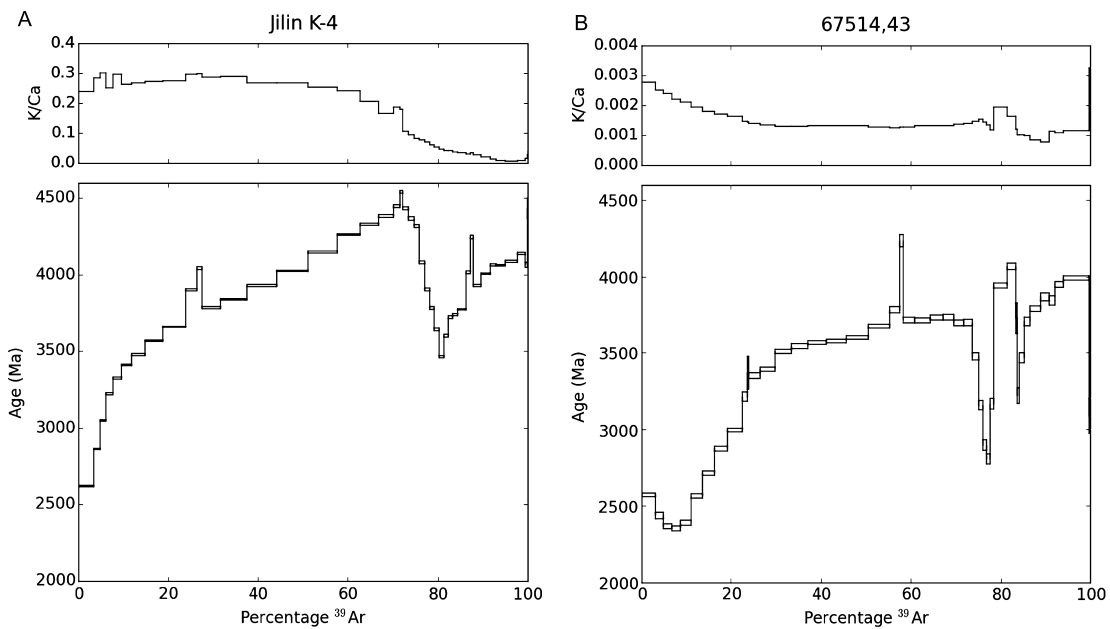
Fig. 2. This figure shows the age spectra and K/Ca for both Jilin K-4 and 67514,43.
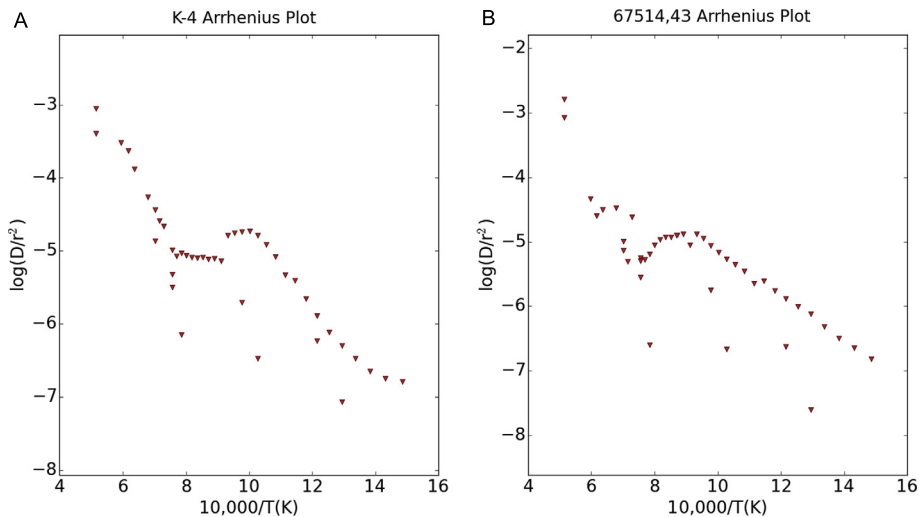

Fig. 3. Arrhenius spectra for both Jilin K-4 and 67514,43. The temperature cycles provide far lower apparent diffusivities than the first heating step at that temperature. This provides further support for the existence of multiple diffusion domains and greatly constrains the activation energies. Uncertainties are much smaller than the symbols and therefore not shown.

that the oldest age in this portion of degassing shows greater ^{40}Ar loss (i.e., has younger ages) than the earlier degassed plagioclase portion is the key observation that plagioclase and clinopyroxene have swapped their relative Ar retentivities between the natural event and laboratory heating.

Our analysis of 67514,43 (Fig. 2B) shows a qualitatively similar age spectrum and Arrhenius plot (Fig. 3B) to that of K-4. However, in contrast with our K-4 analysis, the K/Ca of 67514,43 shows possible evidence for 3 phases. The first phase (K/Ca ≈ 0.003) appears unretentive and is almost completely exhausted at ∼20% ^{39}Ar release, the second (K/Ca ∼ 0.0015) dominates between 20 and 80% ^{39}Ar release, and a third with K/Ca ≈ 0.001. This behavior gives potential evidence for three distinct Ar bearing phases.

4.2. Modeling results

Assuming for the moment that the vacuum degassing data can be directly applied to our samples, we found the top 200 solutions for the K-4 age spectrum are well fit by a reheating event at ∼2.65 Ga (Fig. 4A) with a temperature between 2200 and 2900 K and durations of 300 to 1 μs (Fig. 5A). Our top 10 solutions constrain the heating event to between 2400 and 2800 K with 9 out of 10 again indicating event durations between 50 and 1 μs. Further, the best fit activation energies of 40–50 and 100–120 kcal/mol for the low and high energy phase (Fig. 6A) match well to measured values for Ar diffusion in sodic plagioclase and clinopyroxene (Cassata et al., 2011; Cassata and Renne, 2013), respectively. Finally, the goodness of fit (Fig. 7A) for the Arrhenius spectrum versus that of the age spectrum shows the expected Pareto frontier (see section 2.2).

For 67514,43 the modeling well fits with a heating event at ∼2.3 Ga (Fig. 4B) with temperatures between 2200 and 2800 K and durations of 300 to 1 μs (Fig. 5B), respectively. The top 10 solutions are better constrained to between 2400 and 2800 K and 50 to 1 μs. The activation energies are constrained to between 50–60 and 105–115 kcal/mol (Fig. 6B) for the low and high activation energy phase respectively. Our modeling indicates that both samples experienced similar re-heating events.
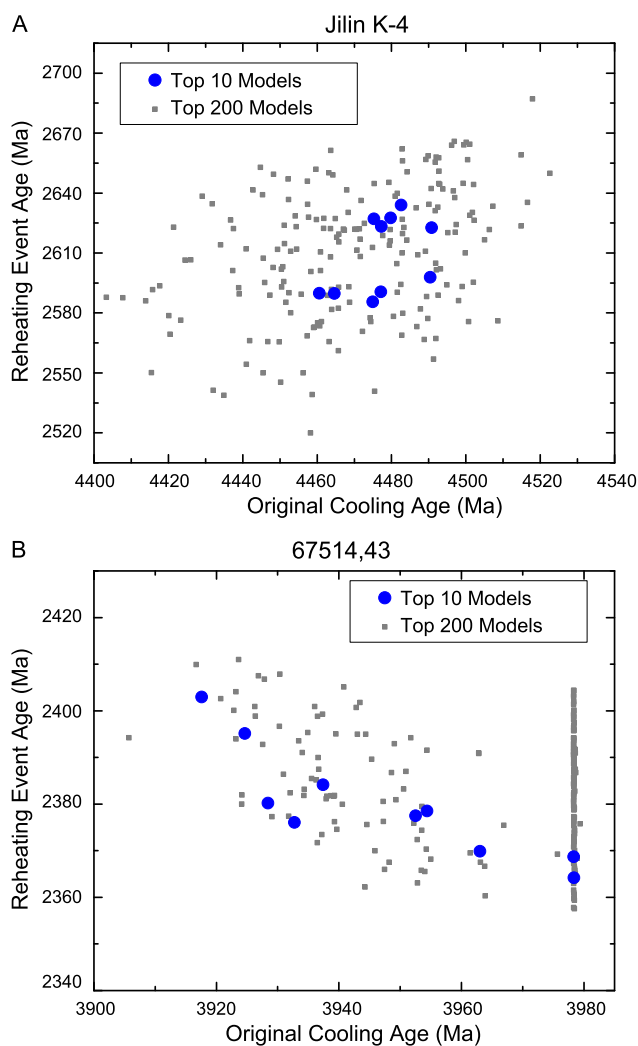
Fig. 4. Figures showing the relationship between the re-heating event age and the original age for the sample based on our model solutions for both K-4 (A) and 67514,43 (B). See Section 3.2 for justification of the cutoff values.
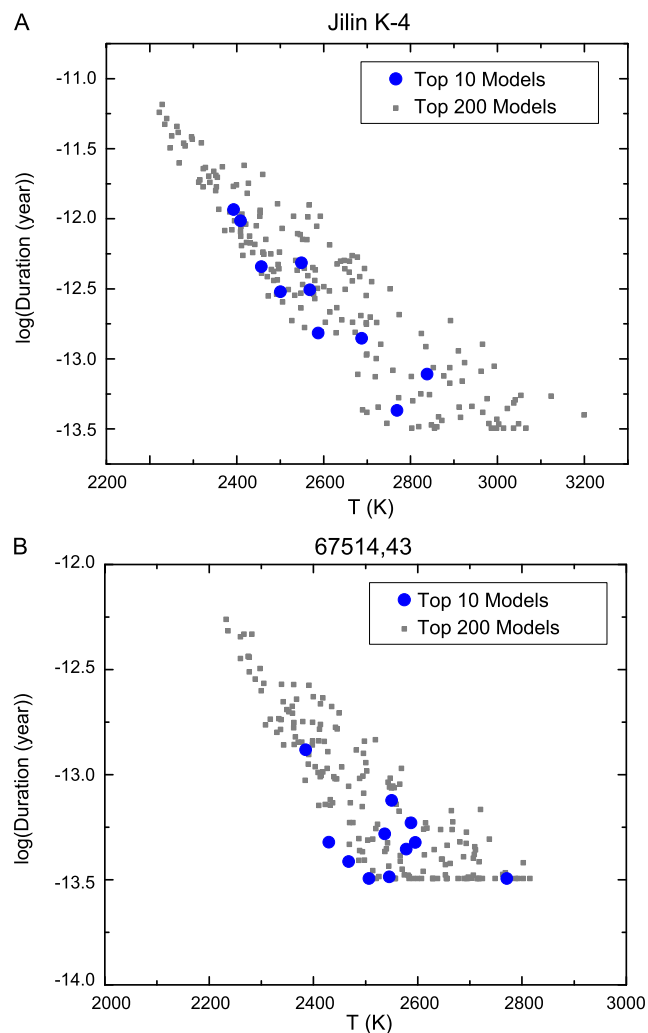

Fig. 5. Figures showing the relationship between modeled duration and intensity of the heating event for both K-4 (A) and 67514,43 (B). See Section 3.2 for justification of the cutoff values.

5. Discussion

5.1. Comparison with previous data

As noted earlier, prior ^{40}Ar/^{39}Ar step-heating results for the Kirin chondrite revealed evidence of multiple thermal events causing extensive diffusive loss of ^{40}Ar (Wang et al., 1980; Harrison and Wang, 1981; cf. Müller and Jessberger, 1985). Due to their strongly contrasting retentivities, feldspars were essentially completely degassed during laboratory heating prior to onset of significant Ar loss from clinopyroxene (Lovera et al., 1997; Cassata et al., 2011) resulting in virtually complete thermal separation of the two Ar release patterns. Wang et al. (1980) noted paradoxically that the clinopyroxene portion of gas release yielded apparently younger ages than the peak of the plagioclase release despite requiring considerably higher temperatures to degas in the laboratory. While our data replicates the broad findings of those studies, we have the advantage of the MDD model which allows us to explore this seemingly paradoxical behavior in detail. This behavior was also noted by Kennedy et al. (2013) in HED meteorites, where plagioclase separates showed older apparent ages than the pyroxene separate.

The apparent reversal of geologic and laboratory degassing behavior was recognized by Harrison and McDougall (1981) in feldspars containing highly retentive excess ^{40}Ar. These authors ar-

gued that excess ^{40}Ar diffused into low E anion vacancies during low temperature heating over millions of years. However, during high temperature laboratory heating, radiogenic and nucleogenic Ar originating in higher E cation sites were lost by diffusion at much greater rates than excess ^{40}Ar which still reside in anion vacancies from which migration is sluggish due to the much lower E. Thus their samples showed an apparent rise to unrealistically old ages (up to 10 Ga) late in laboratory degassing as the excess ^{40}Ar was finally released due to melting. This illustrates the non-intuitive effects of a kinetic crossover where, at low temperatures, one site (or phase) for Ar is less retentive than another but at high temperature (i.e., above the crossover), this behavior is reversed (Fig. 1). A kinetic crossover can also lead to apparent contradictions in an age spectrum where, for example, high temperature gas release (i.e., more retentive sites) yields younger apparent ages than that released at lower temperatures.

Numerical calculations carried out for two domains containing differing activation energies shows dramatically different age spectra depending on whether a thermal event occurred above or below the kinetic crossover (Fig. 1 in Harrison et al., 1991). This prediction was confirmed through analysis of aliquots of natural K-feldspar using different heating schedules. By starting at high temperatures and cycling to lower temperatures (MH-10.cb), Harrison et al. (1991) (see their Fig. 9) were able to produce an essentially flat age spectrum for an originally stair-case type release
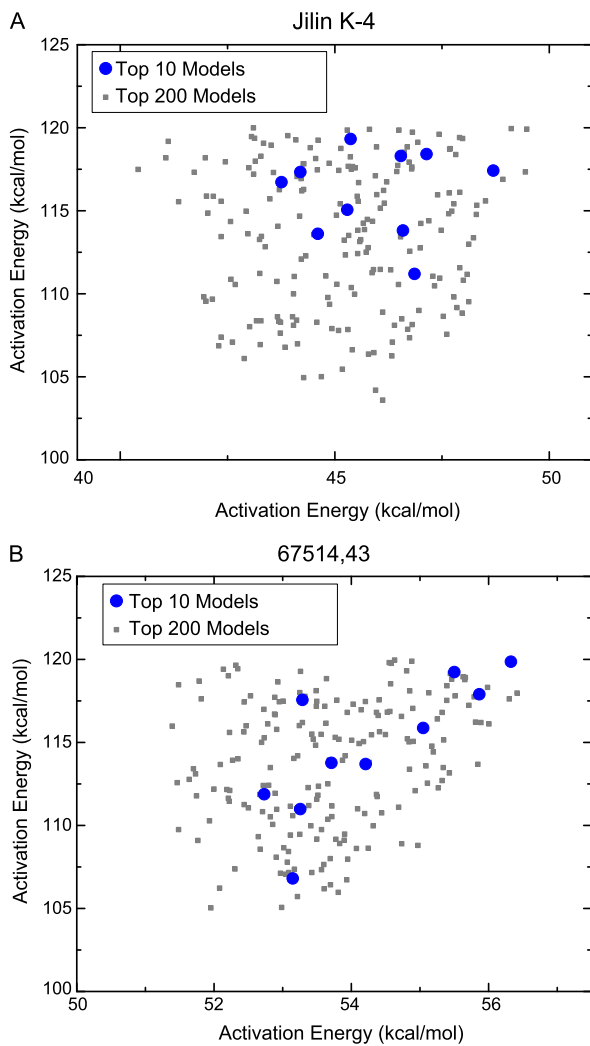
Fig. 6. Figures showing the model activation energies for the two K-bearing phases in K-4 (A) and 67514,43 (B). Note that these results are broadly consistent with plagioclase and clinopyroxene activation energies. See Section 3.2 for justification of the cutoff values.

Fig. 7. Figures showing the goodness of fit to the Arrhenius plot and age spectra for our model solutions. The negative correlation is a manifestation of a Pareto frontier.

pattern. As noted earlier, a specific kinetic crossover between plagioclase and pyroxene was examined to explain $^{40}Ar/^{39}Ar$ analyses of Martian meteorites (Cassata et al., 2010) but ultimately rejected in favor of localized heating of the pyroxene. The above discussion underscores that caution must be taken in both the acquisition and interpretation of results from samples containing multi-activation energies as the laboratory heating schedule can alter the form of an age spectrum. Re-stated, the presence of multiple Ar activation energies dictates that an $^{40}Ar/^{39}Ar$ age spectrum is *a function of both the natural and laboratory heating histories rather than an intrinsic property of the sample.*

5.2. Model fits and kinetic crossover

As shown in Fig. 8A, our best solutions for K-4 produce excellent visual fits to the complex measured age spectrum. We emphasize that this is only possible by accepting fits with temperatures for the ca. 2.6 Ga thermal event over which Ar diffusion in clinopyroxene is faster than that of plagioclase. For example, all of our data was collected at a temperature of <1100 °C while the modeled conditions are >1900 °C suggesting the existence of a kinetic crossover between Ar diffusion in plagioclase and pyroxene. That is, in the natural heating event, clinopyroxene is less retentive of Ar than plagioclase due to the high temperatures of the event.
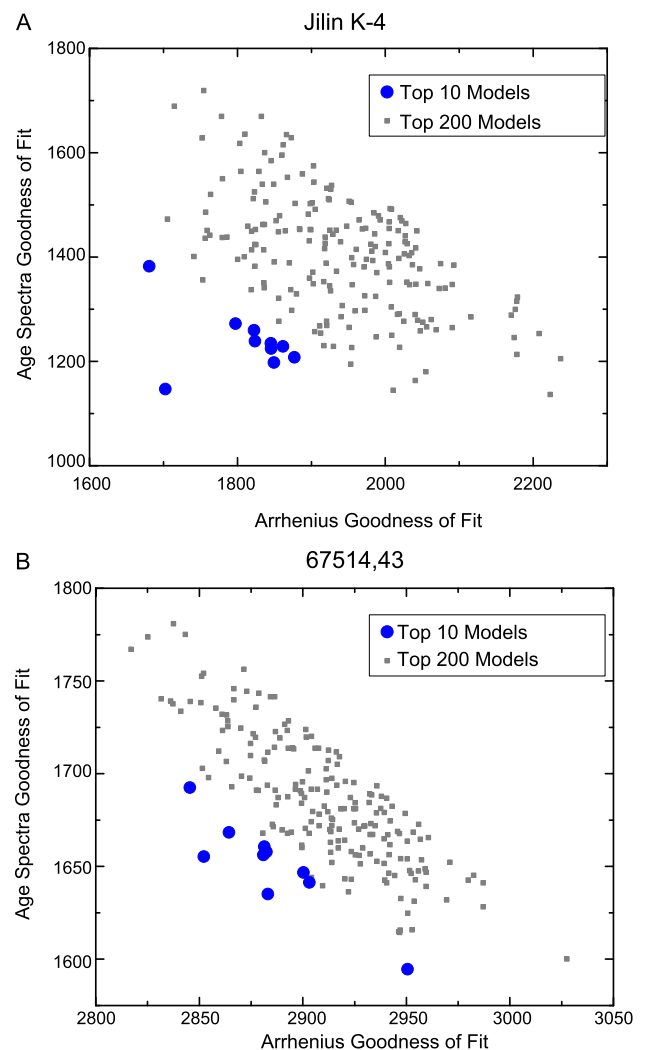
This argument extends to our modeling of 67514,43 suggesting that it also experienced similar conditions. We propose that the laboratory data coupled with a MDD-type model can explain this seeming paradox of the Jilin age spectra without invoking localized pyroxene heating or recoil.

The use of temperature cycles provides the necessary leverage to uniquely fit activation energies for both phases (Fig. 3). Additionally as the cycles release Ar with different age than the steps immediately before and after it, we have altered the appearance of the age spectrum through changing our heating schedule. This further supports the conclusions of Harrison et al. (1991) who demonstrated that the K-feldspar age spectrum can be a function of the laboratory heating schedule provided multiple activations energies are present.

Despite the apparently good fits, in detail the model does not fit the laboratory data within the measured uncertainties. This is an expected result as our diffusion model almost surely underestimates the geometrical complexity of the actual sample (see section 2.2). Going forward with increased computing power, the ability to model more domain sizes should yield ever improving fits to the data. Our modeling also confirms that all apparent heating-step ages underestimate the true rock forming age of this sample (Boehnke et al., 2014). Model fits suggest that the cooling
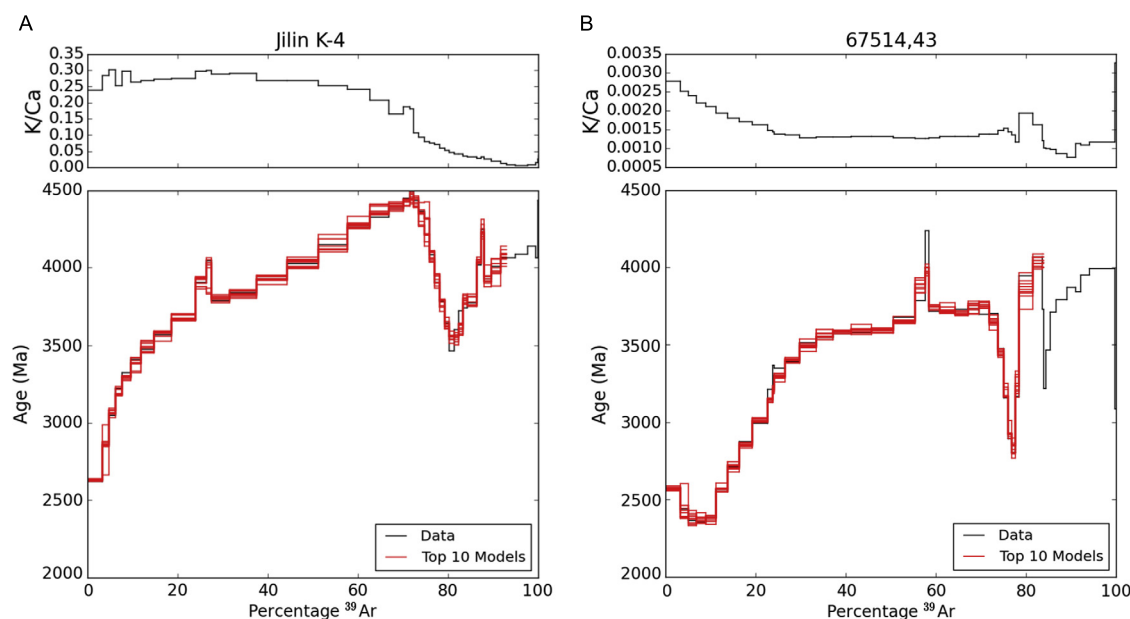
Fig. 8. This shows the top 10 solutions fitted to the age spectrum for each K-4 and 67514,43.

age of the Jilin chondrite is between 4.44 and 4.53 Ga, a range of ∼130 Ma (Fig. 4).

5.3. Shock heating

Cassata et al. (2010) explored the existence of a kinetic crossover for plagioclase and pyroxene through a MDD model but rejected it in favor of a brief, high temperature shock heating event caused degassing of ^{40}Ar from the pyroxene, obviating the need for a kinetic crossover, to interpret ^{40}Ar/^{39}Ar data from Martian meteorites. Based on further work on Ar diffusion in pyroxene, they proposed localized shock heating of pyroxene as an explanation for the age spectrum of Jilin and other meteorites (Cassata et al., 2011). The observation of pyroxene melt veins in ALH84001 (e.g., Barber and Scott, 2006) was seen as support for their interpretation. However, Barber and Scott (2006) also report plagioclase glass indicating that fusion was not limited to pyroxene. That said, we note that melt in both the samples we examined is a minor feature and thus has little or no bearing on the ^{40}Ar systematic.

Since the petrographic evidence is consistent with uniform heating of the entire sample, and thus broadly uniform temperature, the thermal history should be recoverable from an appropriate MDD model. Specifically, we propose that a multi-phase MDD model is fundamentally capable of retrieving shock temperatures from extraterrestrial samples (i.e., a single square-pulse thermal history can adequately and most simply explain the observed data).

Both the model of Cassata et al. (2010) and the present study require relatively rapid post-shock cooling in order to prevent complete diffusive loss of ^{40}Ar. A partial explanation is simply the expected temperature drop of several hundreds of °C following passage of a shock wave. Furthermore, our best fit solutions are a square-pulse equivalent of the actual thermal history implying that calculated peak temperatures are overestimates. Once temperatures have dropped several hundreds of °C below peak values, samples with activation energies for Ar of 40 to 90 kcal/mol cooling exponentially (as expected in the near surface of a parent body) cease to experience significant gas loss. A further consideration to the needed rapid cooling is discussed in detail in the next section.

Given the inherent uncertainties in parent body size and location of the sample within said body, especially after multiple im-

pact events, the size of the resulting body is a major control on the cooling rate as heat diffusion in rock is generally slow. Our solutions require that most of the ^{40}Ar* loss happened during the high temperature heating event and not in the cooling from that event, suggesting a rapid cooling rate. The most plausible mechanism is that our samples resided at the lunar surface or on the exterior of an asteroid, allowing for the fastest possible drop in temperature. While the event we are studying happened at ∼2.6 Ga, cosmogenic nuclides have been interpreted to reflect a complex, multi-stage irradiation history for the Jilin chondrite (e.g., Begemann et al., 1985; Honda et al., 1982) potentially lending supporting the view that sample K-4 resided near the surface over the past ∼2.6 Ga.

The MDD model has rather stringent constraints that may be violated in a shock scenario. The first constraint is that the domain size needs to be set prior to the diffusive loss of radiogenic ^{40}Ar (^{40}Ar*) and maintained until the sample is analyzed in the laboratory. If indeed the MDD model can reconstruct heating due to shockwaves it would suggest that any significant damage is done at the onset of the shockwave rather than at the release. The second requirement is that the sample needs to remain solid throughout the entire process and therefore any post-shock temperatures must be below the zero pressure solidus or result in only minor (i.e., <1%) melting. Note that the confidence gained in assuring that the basic assumptions of the MDD have been met for slowly cooled samples by observing a high degree of correlation between age and Arrhenius spectra (Lovera et al., 1997) is not available for the case of re-heating or for samples containing multiple activation energies.

While disturbed age spectra reveal the loss of ^{40}Ar* prior to laboratory analysis, it doesn't necessarily reveal the loss mechanisms. Given that the ^{40}Ar* closest to a sub- or grain boundary is most readily lost from a sample, if a shockwave is capable of causing ^{40}Ar migration, loss would preferentially occur from the exterior of each domain. Therefore, shock dislocation of ^{40}Ar* could mimic diffusive loss of ^{40}Ar* at high temperatures explaining the fact that the MDD model is capable of excellent visual fits. It remains to be tested whether or not the conditions that are inferred from our inversion indeed reflect shock conditions or are simply a fortuitous feature of shock phenomena.
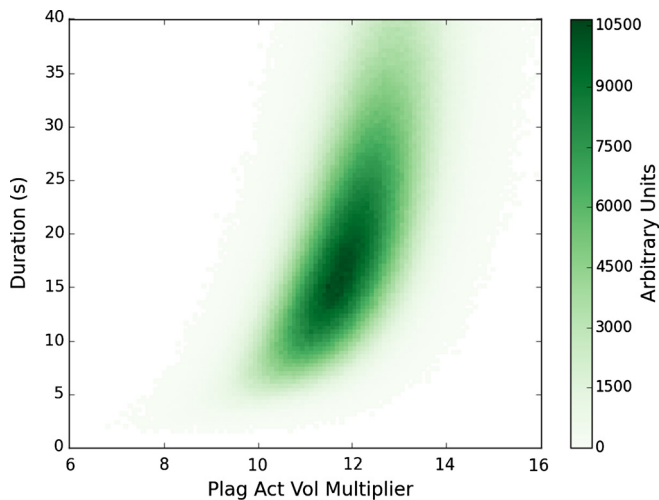
Fig. 9. Figure showing the duration and relative plagioclase activation volume (represented as a multiplier of our assumed pyroxene activation volume of 1 cm^3/mol) for the best fitting solution to the K-4 data at 10 GPa and 1600 K. Our solution here is only one of many which are possible depending on the assumed nature of the shock event and the activation volumes. The color bar represents an unnormalized probability density, that is darker green represents more likely solutions. (For interpretation of the references to color in this figure legend, the reader is referred to the web version of this article.)

5.4. Activation volume effects

While it appears that the best fit model solutions require exceptionally high temperatures and short durations, our modeling to this point has not explicitly included a pressure dependence for the ^{40}Ar* diffusion. That pressure dependence is generally taken as the sum of the reference pressure activation energy (0 GPa for vacuum heating) and the product of pressure and activation volume (ΔV). If the activation volumes of plagioclase and pyroxene are equivalent, then our zero pressure temperature solutions will not change, although the durations become longer. Therefore, using identical ΔV could take our modeled durations of microseconds and increase them to more plausible values for extra-terrestrial shock events (e.g., seconds).

Literature value for the ΔV for dislocation creep and diffusion of trace elements do vary considerably between plagioclase and pyroxene, with the latter, for example, yielding both positive and negative values (Sneeringer et al., 1984; Cherniak and Dimanov, 2010). A further limitation is that most experimental estimates are determined under static pressures of 1 to 2 GPa, far outside our conditions of interest. Thus it is likely that both the durations and temperatures of our solutions are more apparent than real. We constructed an additional model to explore this phenomenon using a Markov Chain Monte Carlo approach (e.g., Boehnke et al., 2015; Gallagher, 2012) as implemented in the emcee python package (Foreman-Mackey et al., 2012). The model was run for a fixed pyroxene ΔV of 1 cm^3/mol at 10 GPa and 1600 K (corresponding to conditions consistent with sample petrology; Stoffler et al., 1991; Xie et al., 2001) and directed to solve for the resulting corrected duration and plagioclase ΔV (represented as a multiple of the pyroxene activation volume). Our modeled solutions (Fig. 9) yield heating durations of 10–20 s at temperatures of ∼1600 K and a plagioclase ΔV of 10–14 cm^3/mol, the latter broadly consistent with literature values (Béjina et al., 2003; Cherniak and Dimanov, 2010) and ΔV for Ar measured in silicates (Harrison et al., 1985, 2009). While this calculated shift in temperature and duration is model dependent, it is, as previously noted, consistent with both petrographic textures and the contrast between pyroxene and plagioclase ΔV measurements (Béjina et al., 2003; Cherniak and Dimanov, 2010). That is to say, our modeling is

purely exploratory and we only seek to demonstrate possible effects of pressure on Ar diffusion in a shock setting. Whether these specific values are borne out by subsequent experiments, there is little question that relating vacuum release Ar data to shock pressures requires that this effect be accounted for.

6. Conclusions

We have shown that highly non-ideal appearing ^{40}Ar/^{39}Ar step-heating data for a sample of the Jilin chondrite (K-4) and an Apollo 16 lunar breccia (67514,43) can be well fit through use of a multi-activation energy and -diffusion domain model coupled to a novel optimization algorithm. This modeling reconciles the apparently younger ages from the clinopyroxene portion late in gas release with the apparently older plagioclase ages in the Jilin K-4 age spectrum. The best fit solutions are for a ∼2.6 Ga shock heating event which reaches ca. 2300 K for microseconds when applying diffusion coefficient obtained in vacuo. When modified using a reasonable contrast in activation volume between constituent minerals to account for the extremely high pressures experienced, the thermal conditions shift to 1600 K for up to tens of seconds. Modeling of an Apollo 16 sample (67514,43) returns a similar thermal history suggesting that brief, high-temperature heating events are a common source for highly irregular ^{40}Ar/^{39}Ar age spectra of extra-terrestrial samples. While our data are consistent with shock heating, further work is needed, both experimentally and analytically, to test the hypothesis that ^{40}Ar/^{39}Ar dating can uniquely recover the conditions of shock heating. In light of these modeling results, we caution against assigning age significance to apparent age spectra from shock heated samples due to the complicated nature of diffusion in multi-activation energy samples, especially at high, transient pressures.

Appendix A. Supplementary material

Supplementary material related to this article can be found online at http://dx.doi.org/10.1016/j.epsl.2016.07.014.

References

Albarède, F., 1978. The recovery of spatial isotope distributions from stepwise degassing data. Earth Planet. Sci. Lett. 39, 387–397.

Barber, D.J., Scott, E.R.D., 2006. Shock and thermal history of Martian meteorite Allan Hills 84001 from transmission electron microscopy. Meteorit. Planet. Sci. 41, 643–662.

Begemann, F., Li, Z., Schmitt-Strecker, S., Weber, H.W., Xu, Z., 1985. Noble gases and the history of Jilin meteorite. Earth Planet. Sci. Lett. 72, 247–262.

Béjina, F., Jaoul, O., Liebermann, R.C., 2003. Diffusion in minerals at high pressure: a review. Phys. Earth Planet. Inter. 139, 3–20.

Boehnke, P., Caffee, M.W., Harrison, T.M., 2015. Xenon isotopes in the MORB source are not distinctive of early global degassing. Geophys. Res. Lett. 42, 4367–4374.

Boehnke, P., Heizler, M.T., Harrison, T.M., Lovera, O.M., Warren, P.H., 2014. Avoiding interpretative pitfalls in analysis of ^{40}Ar/^{39}Ar step-heating data from thermally disturbed meteoritic and lunar samples. In: Proceedings of the 45th Lunar and Planetary Science Conference.

Borg, L.E., Gaffney, A.M., Shearer, C.K., 2014. A review of lunar chronology revealing a preponderance of 4.34–4.37 Ga ages. Meteorit. Planet. Sci. 732, 715–732.

Cassata, W.S., Renne, P.R., 2013. Systematic variations of argon diffusion in feldspars and implications for thermochronometry. Geochim. Cosmochim. Acta 112, 251–287.

Cassata, W.S., Renne, P.R., Shuster, D.L., 2011. Argon diffusion in pyroxenes: implications for thermochronometry and mantle degassing. Earth Planet. Sci. Lett. 304, 407–416.

Cassata, W.S., Shuster, D.L., Renne, P.R., Weiss, B.P., 2010. Evidence for shock heating and constraints on Martian surface temperatures revealed by ^{40}Ar/^{39}Ar thermochronometry of Martian meteorites. Geochim. Cosmochim. Acta 74, 6900–6920.

Cherniak, D.J., Dimanov, A., 2010. Diffusion in pyroxene, mica and amphibole. Rev. Mineral. Geochem. 72, 641–690.

Dalrymple, G.B., Lanphere, M.A., 1971. ^{40}Ar/^{39}Ar technique of K–Ar dating: a comparison with the conventional technique. Earth Planet. Sci. Lett. 12, 300–308.

Dalrymple, G.B., Lanphere, M.A., 1974. ^{40}Ar/^{39}Ar age spectra of some undisturbed terrestrial samples. Geochim. Cosmochim. Acta 38, 715–738.

Deb, K., 2014. Multi-objective optimization. In: Search Methodologies, pp. 403–449.

DeBey, T.M., Roy, B.R., Brady, S.R., 2012. The U.S. Geological Survey's TRIGA reactor.

Dodd, Robert T., 1981. Meteorites: A Petrologic-Chemical Synthesis. CUP Archive.

Dominik, B., Jessberger, E.K., 1978. Early lunar differentiation: 4.42-AE-old plagioclase clasts in Apollo 16 breccia 67435. Earth Planet. Sci. Lett. 38, 407–415.

Dowty, E., Prinz, M., Keil, K., 1974. Ferroan anorthosite: a widespread and distinctive lunar rock type. Earth Planet. Sci. Lett. 24, 15–25.

Fitch, F.J., Hooker, P.J., Miller, J.A., 1976. ^{40}Ar/^{39}Ar dating of the KBS Tuff in Koobi Fora Formation, East Rudolf, Kenya. Nature 263, 740–744.

Foland, K.A., 1974. Ar^{40} diffusion in homogeneous orthoclase and an interpretation of Ar diffusion in K-feldspars. Geochim. Cosmochim. Acta 38, 151–166.

Foreman-Mackey, D., Hogg, D.W., Lang, D., Goodman, J., 2012. Emcee: the MCMC Hammer. Publ. Astron. Soc. Pac. 125, 306–312.

Gallagher, K., 2012. Transdimensional inverse thermal history modeling for quantitative thermochronology. J. Geophys. Res. 117, B02408.

Harrison, T.M., Célérier, J., Aikman, A.B., Hermann, J., Heizler, M.T., 2009. Diffusion of ^{40}Ar in muscovite. Geochim. Cosmochim. Acta 73, 1039–1051.

Harrison, T.M., Duncan, I., McDougall, I., 1985. Diffusion of ^{40}Ar in biotite: temperature, pressure and compositional effects. Geochim. Cosmochim. Acta 49, 2461–2468.

Harrison, T.M., Lovera, O.M., 2014. The multi-diffusion domain model: past, present and future. In: Geological Society, London, Special Publications, pp. 91–106.

Harrison, T.M., Lovera, O.M., Heizler, M.T., 1991. ^{40}Ar/^{39}Ar results for alkali feldspars containing diffusion domains with differing activation energy. Geochim. Cosmochim. Acta 55, 1435–1448.

Harrison, T.M., McDougall, I., 1981. Excess ^{40}Ar in metamorphic rocks from Broken Hill, New South Wales: implications for ^{40}Ar/^{39}Ar age spectra and the thermal history of the region. Earth Planet. Sci. Lett. 55, 123–149.

Harrison, T.M., Wang, S., 1981. Further ^{40}Ar/^{39}Ar evidence for the multi-collisional heating of the Kirin chondrite. Geochim. Cosmochim. Acta 45, 2513–2517.

Heizler, M.T., Perry, F.V., Crowe, B.M., Peters, L., Appelt, R., 1999. The age of Lathrop Wells volcanic center: an ^{40}Ar/^{39}Ar dating investigation. J. Geophys. Res. 104, 767–804.

Honda, M., Nishiizumi, K., Imamura, M., Takaoka, N., Nitoh, O., Horie, K., Komura, K., 1982. Cosmogenic nuclides in the Kirin chondrite. Earth Planet. Sci. Lett. 57, 101–109.

Huneke, J.C., 1976. Diffusion artifacts in dating by stepwise thermal release of rare gases. Earth Planet. Sci. Lett. 28, 407–417.

Jeffery, P.M., Reynolds, J.H., 1961. Origin of excess Xe^{129} in stone meteorites. J. Geophys. Res. 66, 3582–3583.

JIGKMS, 1977. A preliminary survey on the Kirin meteorite shower. Sci. Sin. 20, 502–512.

Jourdan, F., Verati, C., Féraud, G., 2006. Intercalibration of the Hb3gr ^{40}Ar/^{39}Ar dating standard. Chem. Geol. 231, 177–189.

Kennedy, J., Eberhart, R., 1995. Particle swarm optimization. In: Proc. ICNN'95 – Int. Conf. Neural Networks, vol. 4, pp. 1942–1948.

Kennedy, T., Jourdan, F., Bevan, A.W.R., Mary Gee, M.A., Frew, A., 2013. Impact history of the HED parent body(ies) clarified by new ^{40}Ar/^{39}Ar analyses of four HED meteorites and one anomalous basaltic achondrite. Geochim. Cosmochim. Acta 115, 162–182.

Lanphere, M.A., Dalrymple, G.B., 1971. A test of the ^{40}Ar/^{39}Ar age spectrum technique on some terrestrial materials. Earth Planet. Sci. Lett. 12, 359–372.

Lee, J.K.W., 1995. Multipath diffusion in geochronology. Contrib. Mineral. Petrol. 120, 60–82.

Lovera, O.M., 1992. Computer programs to model ^{40}Ar/^{39}Ar diffusion data from multidomain samples. Comput. Geosci. 18, 789–813.

Lovera, Oscar M., Grove, Marty, Harrison, T. Mark, 2002. Systematic analysis of K-feldspar ^{40}Ar/^{39}Ar step heating results II: relevance of laboratory argon diffusion properties to nature. Geochim. Cosmochim. Acta 66 (7), 1237–1255.

Lovera, O.M., Grove, M., Harrison, T.M., Mahon, K.I., 1997. Systematic analysis of K-feldspar ^{40}Ar/^{39}Ar step heating results: I. Significance of activation energy determinations. Geochim. Cosmochim. Acta 61 (15), 3171–3192.

Lovera, O.M., Heizler, M.T., Harrison, T.M., 1993. Argon diffusion domains in K-feldspar II: kinetic properties of MH-10. Contrib. Mineral. Petrol. 113, 381–393.

Lovera, O.M., Richter, F.M., Harrison, T.M., 1989. The ^{40}Ar/^{39}Ar thermochronometry for slowly cooled samples having a distribution of diffusion domain sizes. J. Geophys. Res. 94.

Lovera, O.M., Richter, F.M., Harrison, T.M., 1991. Diffusion domains determined by ^{39}Ar released during step heating. J. Geophys. Res. 96, 2057–2069.

McDougall, I., Harrison, T.M., 1999. Geochronology and Thermochronology by the ^{40}Ar/^{39}Ar Method, second ed. Oxford University Press.

Merrihue, C., Turner, G., 1966. Potassium–argon dating by activation with fast neutrons. J. Geophys. Res. 71, 2852–2857.

Merrihue, C.M., 1965. Trace-element determinations and potassium–argon dating by mass spectroscopy of neutron-irradiated samples. Trans. Am. Geophys. Union 46, 125.

Müller, N., Jessberger, E.K., 1985. Dating Jilin and constraints on its temperature history. Earth Planet. Sci. Lett. 72, 276–285.

Norman, M.D., Duncan, R.A., Huard, J.J., 2006. Identifying impact events within the lunar cataclysm from ^{40}Ar–^{39}Ar ages and compositions of Apollo 16 impact melt rocks. Geochim. Cosmochim. Acta 70, 6032–6049.

Shea, E.K., Weiss, B.P., Cassata, W.S., Shuster, D.L., Tikoo, S.M., Gattacceca, J., Grove, T.L., Fuller, M.D., 2012. A long-lived lunar core dynamo. Science 335, 453–456.

Shuster, D.L., Balco, G., Cassata, W.S., Fernandes, V.A., Garrick-Bethell, I., Weiss, B.P., 2010. A record of impacts preserved in the lunar regolith. Earth Planet. Sci. Lett. 290, 155–165.

Shuster, D.L., Cassata, W.S., 2015. Paleotemperatures at the lunar surfaces from open system behavior of cosmogenic ^{38}Ar and radiogenic ^{40}Ar. Geochim. Cosmochim. Acta 155, 154–171.

Sneeringer, M., Hart, S.R., Shimizu, N., 1984. Strontium and samarium diffusion in diopside. Geochim. Cosmochim. Acta 48, 1589–1608.

Stoffler, D., Keil, K., Scott, E.R.D., 1991. Shock metamorphism of ordinary chondrites. Geochim. Cosmochim. Acta 55, 3845–3867.

Turner, G., 1968. The distribution of potassium and argon in chondrites. In: Ahrens, L.H. (Ed.), Origin and Distribution of the Elements, pp. 387–398.

Turner, G., Cadogan, P.H., 1974. Possible effects of ^{39}Ar recoil in ^{40}Ar–^{39}Ar dating. In: Proceedings of the Fifth Lunar Conference, pp. 1601–1615.

Turner, G., Enright, M.C., Cadogan, P.H., 1978. The early history of chondrite parent bodies inferred from ^{40}Ar–^{39}Ar ages. In: Proceedings of the Lunar and Planetary Science Conference, pp. 989–1025.

Turner, G., Miller, J.A., Grasty, R.L., 1966. The thermal history of the Bruderheim meteorite. Earth Planet. Sci. Lett. 1, 155–157.

Wang, S., McDougall, I., Tetley, N., Harrison, T.M., 1980. ^{40}Ar/^{39}Ar age and thermal history of the Kirin chondrite. Earth Planet. Sci. Lett. 49, 117–131.

Xie, X., Chen, M., Dai, C., El Goresy, A., Gillet, P., 2001. A comparative study of naturally and experimentally shocked chondrites. Earth Planet. Sci. Lett. 187 (3), 345–356.

Zhan, Z., Zhang, J., Li, Y., Chung, H.S., 2009. Adaptive particle swarm optimization. IEEE Trans. Syst. Man Cybern., Part B, Cybern. 39, 1362–1381.